Ion motion in liquid nitrogen

1971 J. Phys. A: Gen. Phys. 4 952

(http://iopscience.iop.org/0022-3689/4/6/023)

J. Phys. A: Gen. Phys., 1971, Vol. 4. Printed in Great Britain

Ion motion in liquid nitrogen

C. S. M. DOAKE and P. W. F. GRIBBON
Department of Physics, University of St. Andrews, Fife, Scotland
MS. received 26th April 1971

Abstract. The mobilities of positive ions in liquid nitrogen have been determined from the transit times of the ions in a triode cell. Two mobilities could be defined from the plots of current against frequency: μ_0 measured in the frame of reference of the cell, and μ_r in that of the liquid. The difference $(\mu_0 - \mu_r)$ was identified with μ_e, a mobility caused by an overall liquid motion induced by the viscous drag of the ions on the liquid. Both our results and earlier ones of Henson, Bruschi, Mazzi and Santini were similar and consistent, and could be explained by the liquid motion theory of Kopylov.

1. Introduction

Discontinuities in the mobilities of ions have been reported in both quantum and classical liquids. In a superfluid much experimental and theoretical work has been done on liquid He II, but in classical liquids the work is more limited; Henson (1964) has reported discontinuities in liquid N_2 and A, and more recently Bruschi *et al.* (1970) reported discontinuities in liquid He I, N_2, A and CCl_4, and Henson (1970) in He I.

Our initial aim was to study the discontinuities in liquid N_2, and to attempt to give a theoretical basis to our observations, because at the time there was not a satisfactory theory for the discontinuities in classical liquids.

The experimental method followed that used in our work on the discontinuities in superfluid He II (Doake and Gribbon 1971). The dc characteristics and ion velocities were studied to get an insight into the behaviour of ions inside a triode cell.

Our results in liquid N_2 do not show discontinuities. Both our results and those of Henson, and Bruschi *et al.*, can be explained by an internal flow or motion of the liquid inside the cell induced by the viscous drag of the ion beam on the liquid.

2. Method of measurement

The method of measuring ion mobilities depended on the determination of the transit time of the ions across a known distance in a cell.

Ions from a radioactive source were introduced into a measuring space across which either a fixed or a variable square wave electric field was applied. Positive ions rather than negative ions were selected since there is less uncertainty about their structure. The ion current was collected, integrated and measured by an electrometer.

The measured ion drift velocity $\langle v \rangle$ in a field E gives the mobility $\mu = \langle v \rangle / E$. Modifications were made to the apparatus used with He II to allow for the much lower mobility $\mu^+ \simeq 10^{-3}\,\mathrm{cm^2\,V^{-1}\,s^{-1}}$ for nitrogen positive ions compared with $\mu^+ \simeq 10\,\mathrm{cm^2\,V^{-1}\,s^{-1}}$ for helium ions. This meant using voltages of several hundred volts applied across a short drift space of about 0·1 cm to give fields E of several kilovolts per centimetre at frequencies down to 1 Hz.

All measurements were made in liquid N_2 at atmospheric pressure. No special precautions were taken against introducing impurities into the liquid, since the results in He II, and in liquid N_2 and A by Bruschi *et al.*, indicated that impurities play a minor role in the mobility of ions.

Two types of cell were used: a triode, with source–grid distance 0·2 cm, grid–collector distance 0·3 cm, and grid mesh 60 lpi; and a slightly larger modified triode, which was designed with three extra guard grids to reduce capacitative pick-up on the collector. Square waves were applied between grid and collector in the triode, and between the first two grids G_1G_2 in the modified four-grid triode.

3. Results

3.1. *DC characteristics*

The dc characteristics in liquid N_2 in the triode were obtained for (i) varying the source–grid field E_{SG} for various constant grid–collector fields E_{GC}, and (ii) varying E_{GC} for various constant E_{SG} values.

These characteristics were similar in shape to those obtained by Dey and Lewis (1968) for liquid A, and by Secker and Lewis (1965) in n-hexane. They were similar also to our dc characteristics in liquid He II for ions at fields below the vortex ring creation field. Both our liquid N_2 and He II characteristics fitted the empirical formula of Januszajtis (1963).

The characteristics of the modified triode were also similar to those for liquid He II, and were consistent with our interpretation of the behaviour within such a cell. Full details of the characteristics of both liquid He II and N_2 will be published later.

We take the similarity of these characteristics to mean that the velocity measurements in liquid N_2 were comparable with those taken in liquid He II, and that our ac results can be interpreted with some confidence.

3.2. *AC characteristics*

We describe our velocity and mobility results for five selected runs, taken for different E_{SG_1} values in the modified triode. In three runs (A, B, C) the forward and reverse square wave fields were the same, and in two runs (D, E) the grid biases were such that the reverse field was three times greater than that of the forward field. The forward and reverse fields are denoted hereafter by E_F and E_R respectively.

3.2.1. *Velocity measurements.* A typical current–frequency, *I–f* graph, with a large low frequency error caused by pick-up, is shown in figure 1. The usual method

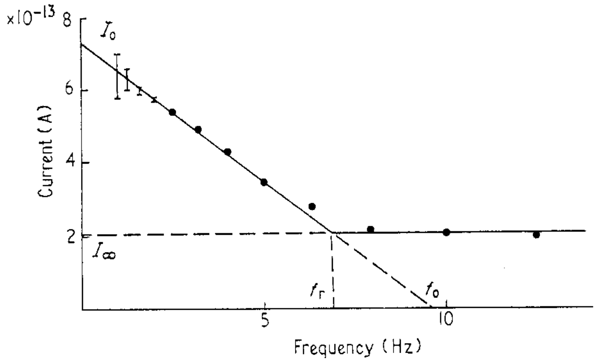

Figure 1. A typical current against frequency graph, with the two lines defining I_0, I_∞, f_r and f_0.

of analysis necessitates drawing a straight line through the low frequency points in figure 1. The transit time across G_1G_2 is derived from the cutoff frequency at which the current becomes zero at high frequencies. This is not possible in liquid N_2, because the current is not zero at the higher frequencies. This is shown in figure 1; the usual straight I–f line holds up to f_r, but at higher frequencies I tends to I_∞, a constant nonzero current for low square wave amplitudes.

In order to show both that the I–f graphs were reliable, and that I_∞ was not spurious but had significance, the current I_0 at $f = 0$ was compared with the direct current I_{DC} for the same forward field. When the fields E_F and E_R were equal, it should be expected from the triode operating equation that $I_0 = \frac{1}{2}I_{DC}$ at $f = 0$. This was confirmed, showing that the cell was operating satisfactorily, and that the I–f graphs could be used to give meaningful mobilities. The field dependences of I_0 and I_∞ for $E_R = 3E_F$ were similar to those for the $E_F = E_R$ runs, and although there could be a pronounced field dependence of I_0 and I_∞, shown for run E in figure 2, this was not inconsistent with normal operation of the cell.

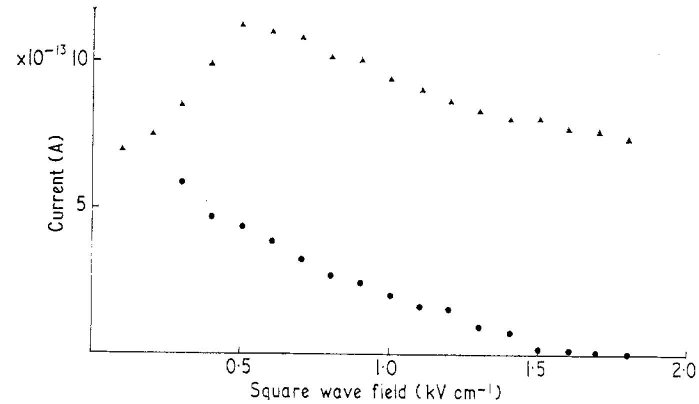

Figure 2. The variation of the currents I_0 ▲ and I_∞ ● with the square wave field for run E.

3.2.2. *Mobility results*. Two mobilities were defined, corresponding to two different cutoff frequencies f_0 and f_r

$$\mu_0 = \frac{2f_0d}{E}$$

$$\mu_r = \frac{2f_rd}{E}$$

where f_0 was the cutoff frequency from an extrapolation of the linear portion of the I–f graph to $I = 0$ in figure 1, f_r the frequency above which I became independent of frequency, d the spacing and E the field between G_1 and G_2.

All the values of μ_0 and μ_r as a function of field are plotted for the runs A–E in figures 3 and 4 respectively. The relative error in each mobility reading for a particular run was 5% and came from the uncertainty in the values of f_0 and f_r estimated from the I–f graphs: the absolute error in mobility for a given run was about 10%. The scatter in mobility values from one run to another was about 20%. All the runs showed the same behaviour of μ_0 with field, but μ_r showed a slight decrease with

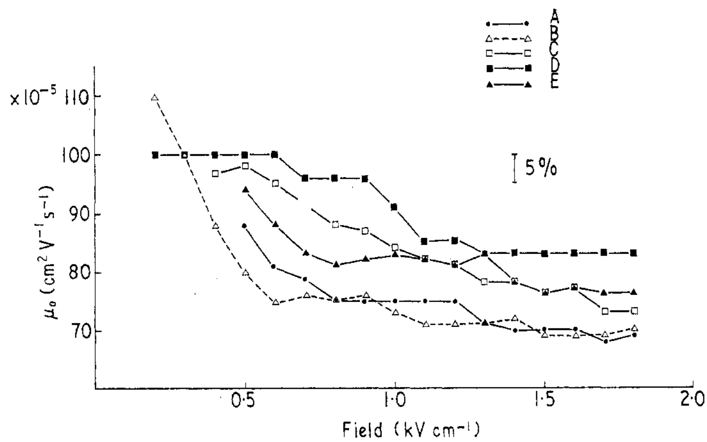

Figure 3. The variation of μ_0 with field for the runs A–E.

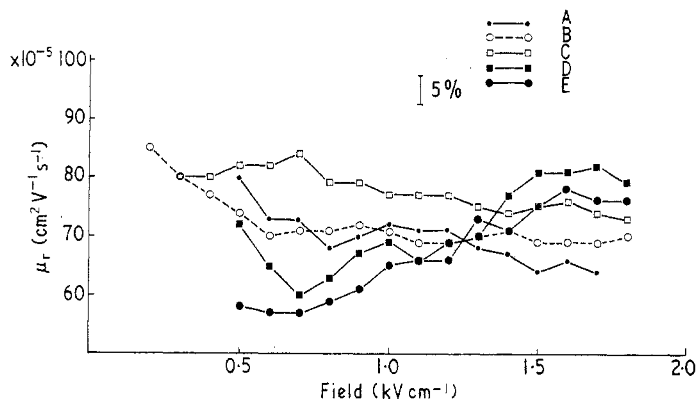

Figure 4. The variation of μ_r with field for the runs A–E.

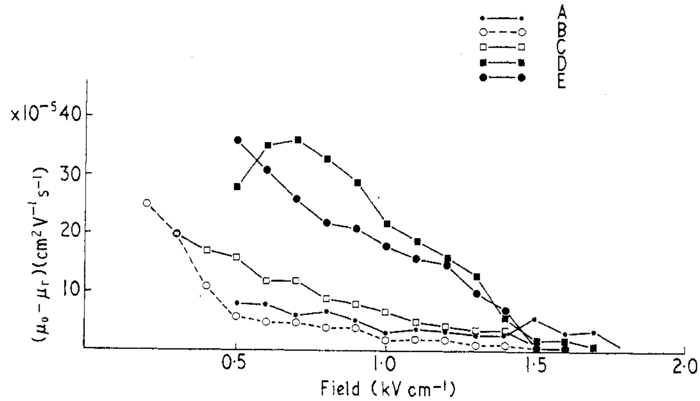

Figure 5. The mobility difference ($\mu_0 - \mu_r$) against field for the runs A–E.

field in runs A, B and C, and a slight increase in runs D and E. The behaviour of μ_r with field for an individual run seemed to be outside our limits of error, while the scatter from one run to another was just inside our estimated error.

The values of the difference in mobility $(\mu_0 - \mu_r)$ for each run are plotted in figure 5. It can be seen that despite the difference in behaviour of μ_r between runs, the function $(\mu_0 - \mu_r)$ has the same qualititative behaviour for each run, but with runs A, B and C falling into one group (1), and runs D and E into another group (2). This will be discussed later.

The validity of our results can be checked by making a comparison with the other results reported by Henson, and Bruschi *et al.*

Our average values for positive ions were $\mu_r = 7{\cdot}1 \times 10^{-4}$ cm^2 V^{-1} s^{-1}, and $\mu_0 = 10{\cdot}5 \times 10^{-4}$ cm^2 V^{-1} s^{-1}. This μ_0 value agreed with that of Bruschi *et al.*, who used a radioactive source of the same strength and a current approximately equal to 10^{-12} A of the same magnitude. Our value and that of Bruschi *et al.* were a factor of 3 lower than Henson's low field value of $2{\cdot}5 \times 10^{-3}$ cm^2 V^{-1} s^{-1}, but it is suggested later that this discrepancy arose because of the higher currents of about 10^{-9} A and gating fields of approximately 5 kV cm^{-1} that had to be used by Henson in his field emission tungsten tip technique.

Our triode square wave method of measuring ion velocities in liquid N_2 also had certain advantages over the methods of Henson, and Bruschi *et al.*, which analysed the transit time of a unidirectional current pulse moving through the liquid. The main advantage was that the two mobilities μ_0 and μ_r can only be defined easily in a triode where the zero of current is well known. Their pulse methods measured the time for the edge of a current pulse to fall to an equilibrium, and possibly nonzero, current value, and gave a mobility value equivalent to our μ_0.

4. Liquid motion

Some evidence for ion induced liquid motion will be given here, and then applied in § 5 and § 6 to the analysis and discussion of our results.

In classical liquids the motion of ions under the influence of an electric field will cause liquid motion in the direction of ion motion, and the amount of liquid motion will depend on the liquid viscosity η, the electrical energy input to the cell, and the cell dimensions. The liquid motion will increase the ion velocity and given an anomalously high mobility measurement.

There is both direct and indirect evidence for liquid motion. For example, liquid motion caused by ionic conduction in an insulating liquid can create pressures of a fraction of an atmosphere, and this has been used in the construction of 'ion-drag' pumps by Stuetzer (1960). The most direct evidence is the visual observation of liquid motion in hexane made by Gray and Lewis (1965), who found that the liquid in a cell could attain a velocity of about 1 cm s^{-1}, a value comparable in magnitude with the drift velocity of the ions in the applied electric field. A marker dye, injected into a cell carrying a small current of about 10^{-11} A, was seen to move in a field-free region of the cell, showing that the motion was not caused by ions trapped in the dye.

Liquid motion has been used also to explain ion mobility results in n-hexane by Secker and Lewis (1965), and in liquid A by Dey and Lewis (1968). Their results gave μ values higher than expected, showing a decrease in low field μ as the steady state cell current decreased. They were found to be in qualitative agreement with a theory by Kopylov (1964), which related the liquid velocity v_e to the current I and field E in a cell, according to

$$v_e = A_1 E \ln \frac{A_2 I}{E} \tag{1}$$

where A_1 and A_2 were constants, which depended on the liquid properties and the cell dimensions.

The effect of liquid motion on the measured μ values is as follows. If the real ion velocity with respect to the liquid is v_r, and the liquid itself is moving at v_e in the cell, then the ion velocity measured in the fixed frame of reference of the cell is v_0, so that $v_0 = v_r + v_e$. Since liquid motion only alters the reference frame, the mobilities are additive and this means that the measured mobility is greater than the real mobility by the additional term for the liquid mobility.

5. Analysis of results

We will use Kopylov's theory to explain our ion mobility results, but first we must indicate the conditions under which they were obtained in order to use the valid equations of the theory.

Our mobilities were obtained under low field conditions. This implies that the energy, $eE\lambda$, gained by an ion of charge e in the field E per mean free path λ was less than the ion's thermal energy kT, with the result that the motion of the ions was controlled by classical kinetic theory, and that Stoke's law for μ could be used, that is, $\mu = e/6\pi\eta R$, where R is the ion radius. This mobility μ is independent of the field E, and we identify it with the real mobility. Any field dependence of the measured mobility μ_0 was assumed therefore to come from the field dependence of the liquid motion. Low field conditions allow Kopylov's equation (1) to be applied to our results.

Liquid motion was responsible for the behaviour in our velocity measuring cell, and showed up in the I–f graphs. For example, the finite nonzero current I_∞ existed because the liquid always carried some current through the cell to the collector at any square wave frequency, and on the reverse half of the wave the ions had a smaller velocity relative to the cell than for the forward cycle and therefore not all the ions returned to the grid.

Our mobilities, defined as μ_r and μ_0, were identified with the real mobility with respect to the liquid and the measured mobility with respect to the cell respectively. μ_r was given when the square wave current reached I_∞, and μ_0 when the extrapolated I–f line reached $I = 0$. Since μ_r and μ_e were additive, and using v_e defined by equation (1), it follows that

$$\mu_0 - \mu_r = \mu_e = \frac{v_e}{E} = A_1 \ln \frac{A_2 I}{E}. \tag{2}$$

In the analysis of our results we have assumed a constant current I, and modified equation (2) to

$$\mu_0 - \mu_r = C_1 \ln \frac{C_2}{E} \tag{3}$$

where $C_1 = A_1$ has the dimensions of mobility, and $C_2 = A_2 I$. Both C_1 and C_2 are assumed to be constant and independent of the field E in a given run.

We fitted equation (3) to the results for $(\mu_0 - \mu_r)$, given in figure 5, (*a*) for each individual run, and (*b*) for the group (1) runs and (*c*) for the group (2) runs. We used a multiple linear regression analysis to obtain the values for C_1 and C_2 with their standard errors given in table 1. There is good agreement between the theory and the experiment with our results falling into the two distinct groups (1) and (2) as expected. The C_1 and C_2 values derived from the work of Henson, and Bruschi *et al.*, are included for comparison and are discussed in § 7.

Table 1

Run	$C_1 \times 10^5$ ($cm^2\ V^{-1}\ s^{-1}$)	$C_2 \times 10^{-3}$ ($V\ cm^{-1}$)	Correlation coefficient
1 A	$6{\cdot}2 \pm 1{\cdot}6$	$2{\cdot}30 \pm 0{\cdot}07$	0·76
1 B	$12{\cdot}3 \pm 1{\cdot}2$	$1{\cdot}26 \pm 0{\cdot}04$	0·94
1 C	$11{\cdot}8 \pm 0{\cdot}3$	$1{\cdot}75 \pm 0{\cdot}01$	0·99
2 D	$37{\cdot}0 \pm 5{\cdot}0$	$1{\cdot}70 \pm 0{\cdot}04$	0·91
2 E	$30{\cdot}3 \pm 1{\cdot}6$	$1{\cdot}72 \pm 0{\cdot}02$	0·98
1 (average)	$12{\cdot}3 \pm 0{\cdot}9$	$1{\cdot}50 \pm 0{\cdot}05$	0·89
2 (average)	$34{\cdot}5 \pm 2{\cdot}3$	$1{\cdot}70 \pm 0{\cdot}03$	0·94
Average, 1 + 2	$14{\cdot}7 \pm 0{\cdot}2$	$1{\cdot}97 \pm 0{\cdot}02$	0·99
Henson	54 ± 5	$9{\cdot}8 \pm 0{\cdot}2$	
Bruschi *et al.*	5·4	4·1	for $\mu_r = 7 \times 10^{-4}\ cm^2\ V^{-1}\ s^{-1}$
		1·7	for $\mu_r = 9{\cdot}57 \times 10^{-4}\ cm^2\ V^{-1}\ s^{-1}$
		4·0	for $\mu_r = 8{\cdot}1 \times 10^{-4}\ cm^2\ V^{-1}\ s^{-1}$

6. Discussion

The C_1 and C_2 values are discussed with reference to the field conditions in our cell during each run, and they are shown to be consistent with the concept of liquid motion within the cell.

Table 1 shows that while C_2 was approximately constant for each run, C_1 which is a measure of the mobility μ_e, showed a significant difference between the runs of groups (1) and (2). The theory indicates that the liquid velocity is determined both by the magnitude of the current I, through C_2, and on the characteristic time taken for an equilibrium velocity to be set up for a given current. In the triode cell the average current depends on the frequency; where although the magnitude of the current in each frequency pulse is constant, the time average of the current, and so C_2, is a decreasing function of the square wave frequency. However, if the characteristic time to set up a flow pattern is greater than the square wave period, C_2 becomes independent of the frequency dependent current but proportional to the equivalent direct current. Our results, which showed a slight difference in the C_2 values between each run, were interpreted to show that there was a small dependence on the magnitude of the equivalent dc, and the small error in C_2 in an individual run was interpreted to show that there had been sufficient time for liquid motion to have been set up by the current flow.

The effect of the field on the liquid velocity and mobility is shown by the marked difference in the C_1 values for the groups (1) and (2) runs. The group (1) runs were taken when the forward and reverse fields were equal, and the group (2) runs when $E_R = 3E_F$; the C_1 values for group (1) runs were three times those for the group (2) runs.

We explain this difference by associating C_1 with the liquid motion; and suggest that the flow pattern is different in the two groups due to the behaviour of v_e and μ_e with field. This behaviour is shown in figure 6, which has been plotted using equation (1) and our C_1 and C_2 values for the average of groups (1) and (2). v_e has a maximum velocity $v_e \simeq 0{\cdot}1$ cm s^{-1} at $E \simeq 700$ V cm^{-1}. For higher fields, v_e is a decreasing function of E, agreeing with the results quoted by Kopylov.

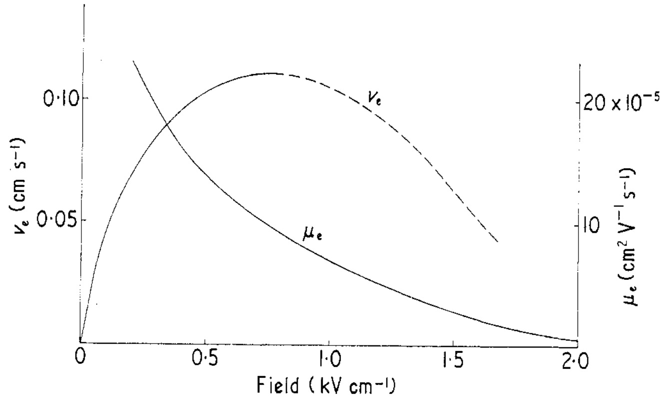

Figure 6. The liquid velocity and mobility, v_e and μ_e, as functions of field, from the theory of Kopylov, and using our experimental parameters.

The development of the liquid motion can be outlined for different square wave fields. The liquid motion in the measuring space is induced initially by the forward motion of the ions due to E_F, but in the reverse half of the cycle the motion is reduced by ions still in the measuring space travelling back to the grid. When $E_R > E_F$, the reduction in liquid motion in the forward direction was lower than when $E_R = E_F$ because μ_e is lower in E_R than in E_F. The extracting field in the source–grid space also contributes to the forward liquid motion and this motion could be expected to continue through the grid into the measuring space. The liquid motion also depends on the time during which a current is passed, a forward motion occurring for a time τ_F equal to the half period $T/2$ of the square wave and a reverse motion during the shorter time τ_R taken to empty the measuring space. For square wave frequencies beyond the cutoff frequency, τ_F/τ_R depends on E_F/E_R; a high reverse field $E_R > E_F$ causes a smaller decrease in the forward liquid motion than for $E_R = E_F$, and gives a correspondingly higher C_1 value. This process for the growth of liquid motion does not depend strongly on the characteristic time τ when $\tau > T$, since a time average over any number of square wave periods will always induce a quasiequilibrium liquid velocity.

Our analysis has concentrated on the difference $(\mu_0 - \mu_r)$ and has been shown to be consistent with liquid motion. However, there are certain criticisms in this approach: for example, the slight field dependence of the assumed field independent μ_r cannot be explained, and this tends to question whether the absolute mobility values can be defined by the μ_r and μ_0 values of our *I–f* graphs.

7. Relevance to other mobility results

We can now discuss the results of Henson and Bruschi *et al.* for positive ions in liquid N_2, and indicate how liquid motion may be involved in their observations.

Henson (1964) plotted his mobility as a function of electric field. He drew (see for example, his figure 15) a line connecting each experimental point and obtained a series of constant mobility levels, the changes to a new level occurring at fields which had no simple relationship to each other. We analysed his results using equation (1) and obtained the C_1 and C_2 values given in table 1. His C_1 value was greater than our C_1 value, but a high value of this measure of the ion mobility was not unexpected since his pulse method not only provided a forward liquid motion but his higher source–grid fields also contributed to the forward liquid motion. His C_2 value was larger and quantitatively in rough agreement with the value expected for the larger current of about 10^{-10} A used in his experiment. We therefore suggest that his overall field dependence of mobility may be explained in the same way as ours by liquid motion.

The results of Bruschi *et al.* (1970) in liquid N_2 at 1·8 atmosphere pressure were fitted also to Kopylov's theory. Their mobility values were our μ_0, and the overall field dependence of mobility was taken from their figure 1. Their C_1 value was the slope of their curve, plotted as μ against ln E, and their C_2 value in units of V cm^{-1} were calculated for three μ_r values: our $\mu_r = 7\times10^{-4}$ cm^2 V^{-1} s^{-1} gave one of the C_2 values; our $C_2 = 1{\cdot}7\times10^3$, a value chosen since our cell geometry and current were similar to those of Bruschi *et al.*, gave $\mu_r = 9{\cdot}57\times10^{-4}$ cm^2 V^{-1} s^{-1}. This latter μ_r value is in good agreement with the low field results quoted by Bruschi *et al.*, but it meant that liquid motion gave a negative contribution to mobility at high fields. The third value $\mu_r = 8{\cdot}1\times10^{-4}$ cm^2 V^{-1} s^{-1} was obtained for a value of $C_2 = 4\times10^3$, and was in agreement with their high field mobility values. These C_1 and C_2 values can be interpreted as follows: firstly, the small C_1 value was taken to mean that liquid motion had less effect in their cell, and secondly, the various C_2 and μ_r values are quoted to provide full information, but the crudeness of the fit of their data to the theory and the unknown pressure dependence of mobility does not permit us to draw detailed conclusions from them.

8. Relevance to mobility discontinuities

Both Bruschi *et al.* (1970) and Henson (1970) reported sharp changes or discontinuities in mobility in classical liquids.

Henson (1970) determined the low-field mobility of positive ions in He I using the same technique that he used in liquid N_2, and found $\mu \simeq 6{\cdot}5\times10^{-2}$ cm^2 V^{-1} s^{-1}, while Bruschi *et al.* (1970) also in He I found $\mu \simeq 3{\cdot}5\times10^{-2}$ cm^2 V^{-1} s^{-1}. Henson found that his technique often gave more than one transit time for a given field, and this fact, added to the discrepancy in the mobility values, indicates that his measuring technique was causing liquid motion. This conclusion is strengthened by the fact that he worked with fields up to 7 kV cm^{-1} and beyond the critical field of about 5 kV cm^{-1} needed by Bruschi *et al.* to detect their first discontinuity. Since the field dependence of Henson's mobility levels is not available, it has not been possible to analyse his results further for evidence of liquid motion. His explanation for discontinuities was that there were changes in the effective cross section of the ions caused by a clustering of additional polarized atoms at the surface of the ions.

Bruschi *et al.* used low current densities, since they realized that liquid motion was possible, but they did not test for it. However, since both their and our current densities were similar, it is likely that their results were affected also by liquid motion.

Liquid motion would give a scatter in the measured μ values. If the measurements were always taken in a systematic fashion, for example, with increasing E, then the discontinuities could appear in a regular sequence that depended on the time taken between each individual measurement. This follows from the time scale for any stable liquid flow pattern that has been set into motion in the cell, since such a flow could take either a long time to decay or to change to another flow pattern.

The appearance of discontinuities is intimately related to liquid motion. When the ions reach an equilibrium drift velocity in an electric field they lose momentum through scattering and transferring energy to the background fluid. Although some of the energy loss by the ions can be dissipated as heat, it can also transfer momentum to the fluid so that a force or pressure gradient will be set up in the fluid in the direction of ion motion. An overall motion of the fluid therefore takes place, and its magnitude will depend on the relative importance of the elastic and inelastic ion–fluid scattering probabilities. The discontinuities would occur when the ions have an increased interaction with the fluid, and the increased momentum loss rate of the ions would give a corresponding momentum gain or motion to the fluid.

The interactions between ions and the fluid background depend on both the energy and momentum transfer mechanisms and on their dependence on the ion velocities and the applied fields. However, the classical kinetic theory description of ion mobility can only discuss the interaction in terms of a collision cross section and does not take into account the full interaction of the ions with the background fluid. An analysis which considers the role of the background fluid in more detail would be a fruitful approach towards a better understanding of the effect of liquid motion in mobility experiments.

References

Bruschi, L., Mazzi, G., and Santini, M., 1970, *Phys. Rev. Lett.*, **25**, 330–3.
Dey, T. H., and Lewis, T. J., 1968, *J. Phys.* D: *Appl. Phys.*, **1**, 1019–29.
Doake, C. S. M., and Gribbon, P. W. F., 1971, *J. Phys.* C: *Solid St. Phys.*, in the press.
Gray, E., and Lewis, T. J., 1965, *Br. J. appl. Phys.*, **16**, 1049–50.
Henson, B. L., 1964, *Phys. Rev.*, **135**, A1002–8.
—— 1970, *Phys. Rev. Lett.*, **24**, 1327–9.
Januszajtis, A., 1963, *Acta Phys., Polonika*, **24**, 809–16.
Kopylov, G. N., 1964, *Sov. Phys.–Tech. Phys.*, **8**, 962–8.
Secker, P. E., and Lewis, T. J., 1965, *Br. J. appl. Phys.*, **16**, 1649–56.
Stuetzer, O. M., 1960, *J. appl. Phys.*, **31**, 136–46.